

## **NON-LINEAR VIBRATIONS OF AXIALLY MOVING ORTHOTROPIC WEB**

Krzysztof Marynowski  
Technical University of Łódź  
Department of Machines Dynamics  
Stefanowskiego 1/15, 90 - 924 Łódź, Poland  
Tel. (42) 6312230, E-mail: [kmarynow@ck-sg.p.lodz.pl](mailto:kmarynow@ck-sg.p.lodz.pl)

### **Abstract**

A new approach to analysis of the dynamic behaviour of axially moving orthotropic web is presented. In this paper the numerical method of Unger's transition matrix and Godunov's orthogonalization procedure are used to solve the non-linear problem of axially moving system. The results of numerical investigations show the solutions of the linearized and non-linear problems. Free vibrations of the steel web in subcritical and supercritical regions of transport speed are analyzed.

### **1. Introduction**

Axially moving webs in the form of thin flat rectangular shape materials with small flexural stiffness one can find in industry as band saws blades, power transmission belts, magnetic tapes and paper webs. Excessive vibrations of moving webs increase defects and can lead to failure of the web. The analysis of vibration and dynamic stability of such systems is very important for design of manufacturing devices.

A lot of the earlier works in this field focused on dynamic investigations of string-like and beam-like axially moving isotropic systems (e.g. [3], [4]). In the case of a two-dimensional, axially moving thin web, the exact dynamic solutions, satisfying the non-linear, coupled equations governing the web's motion, probably cannot be determined in a closed form. Recent works analysed equilibrium displacement, stress distribution in non-linear model of axially moving web [5], the wrinkling phenomenon and stability of linear model of axially moving isotropic plate ([6], [7]), stress distribution in axially moving plate [2] and non-linear vibrations of power transmission belts [8].

It is well known that many materials traditionally considered as isotropic exhibit some degree of anisotropy due to working processes. Also growing interest in composite materials demands a better understanding of the strength of materials anisotropic by design. The aim of this paper is to analyse the non-linear vibrations of axially moving orthotropic web. The differential equations of motion are derived from the Hamilton's principle taking into account the Lagrange's description, the strain Green's tensor for thin-walled plates and the Kirchhoff's stress tensor.

The linear problem of axially moving orthotropic web dynamic behaviour has been solved in [9]. In this paper the numerical method of Unger's transition matrix and Godunov's orthogonalization procedure are used to solve the non-linear problem.

One of the principal goals of the numerical analysis is to investigate dynamic behaviour of axially moving steel web in subcritical and supercritical regions of transport speed. Numerical investigations have been carried out for thin orthotropic steel plate.

## 2. Mathematical model of the moving web system

An elastic moving web of the length  $l$  is considered. The web moves at velocity  $c$  which may change in time. The co-ordinates system and geometry are shown in Fig. 1.

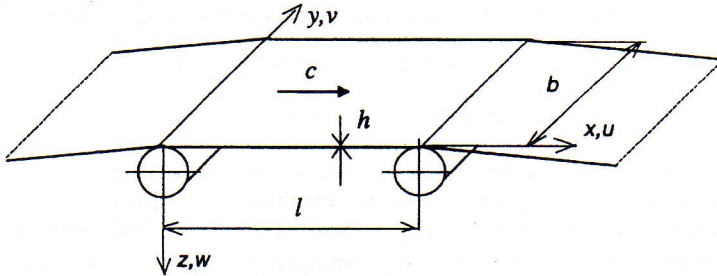


Fig. 1. Axially moving web

The dynamic analysis is carried out using the thin-walled plate model. The considered web is composed of plane rectangular plate segments of principal axes of orthotropy parallel to their edges. Such model enables dynamic analysis of the web with various material properties and parameters. The governing equations of motion for the  $i$ -th plate segment were derived in [9] and have the following form:

$$\rho_i h_i (-w_{i,tt} - 2cw_{i,x} - c_x w_{i,x} - c^2 w_{i,xx}) - \beta_i w_{i,t} - \beta_i c w_{i,x} + M_{xi,xx} + 2M_{xyi,xy} + M_{yi,yy} + q_i + (N_{xi} w_{i,x})_{,x} + (N_{yi} w_{i,y})_{,y} + (N_{xyi} w_{i,x})_{,y} + (N_{xyi} w_{i,y})_{,x} = 0 \quad (1)$$

$$\rho_i h_i (-u_{i,tt} - c_x - 2cu_{i,x} - c_x u_{i,x} - c^2 u_{i,xx}) - \beta_i c - \beta_i u_{i,t} - \beta_i cu_{i,x} + N_{xi,x} + N_{xyi,y} = 0 \quad (2)$$

$$\rho_i h_i (-v_{i,tt} - 2cv_{i,x} - c_x v_{i,x} - c^2 v_{i,xx}) - \beta_i v_{i,t} - \beta_i cv_{i,x} + N_{xyi,x} + N_{yi,y} = 0 \quad (3)$$

where:  $N_{xi}$ ,  $N_{yi}$ ,  $N_{xyi}$  - in-plane stress resultants for the  $i$ -th plate,

$q_i$  - transverse loading of the  $i$ -th plate,

$u_i$ ,  $v_i$ ,  $w_i$  - displacement components of the  $i$ -th plate middle surface,

$\beta_i$  - damping coefficient,

$\rho_i$  - mass density of the  $i$ -th plate.

Neglecting the phenomenon of elastic waves propagation in the  $x - y$  plane for  $c = 0$  and  $t = \text{const}$  the governing equations (2) and (3) one can replace by the non-linear compatibility equation in the following form

$$\frac{1}{E_i h_i \eta_i} \left[ \Phi_{i,xxxx} + \Phi_{i,xyxy} \left( \frac{E_i \eta_i}{G_i} - 2\nu_i \eta_i \right) + \eta_i \Phi_{i,yyyy} \right] = w_{i,xy}^2 - w_{i,xx} w_{i,yy} \quad (4)$$

where:  $\Phi$  - the Airy stress function, which satisfy the conditions

$$N_{xi} = \Phi_{i,yy}; \quad N_{yi} = \Phi_{i,xx}; \quad N_{xyi} = -\Phi_{i,xy} \quad (5)$$



After substituting (5) into (1) the non-linear mathematical model of the moving web system has the following form

$$\rho_i h_i (-w_{i,tt} - 2cw_{i,xt} - c_{,t} w_{i,x} - c^2 w_{i,xx}) - \beta_i w_{i,t} - \beta_i c w_{i,x} + M_{xi,xx} + 2M_{xyi,xy} + M_{yi,yy} + q_i + \Phi_{i,yy} w_{i,xx} - 2\Phi_{i,xy} w_{i,xy} + \Phi_{i,xx} w_{i,yy} = 0 \quad (6)$$

$$\frac{1}{E_i h_i \eta_i} \left[ \Phi_{i,xxxx} + \Phi_{i,xyy} \left( \frac{E_i \eta_i}{G_i} - 2\nu_i \eta_i \right) + \eta_i \Phi_{i,yyyy} \right] = w_{i,xy}^2 - w_{i,xx} w_{i,yy} \quad (7)$$

The kinematics and static continuity conditions at the junctions of adjacent plates are given in [9].

### 3. Solution of the problem

The exact dynamic solutions satisfying the non-linear, coupled equations (6), (7) probably cannot be determined in closed form. Below the non-linear analysis on the base of an approximate analytical solution is presented. To simplify applied notations the plate segment subscript  $i$  is omitted in further considerations. One assumes that the plate (strip) is tensioned only in its longitudinal direction, hence

$$N_{x0}(y) \neq 0; \quad N_{y0} = N_{xy0} = 0; \quad (8)$$

The boundary conditions referring to the simple support of the web at both ends are

$$w(x=0, y) = w(x=l, y) = 0; \quad (9)$$

$$M_y(x=0, y) = M_y(x=l, y) = 0$$

The steady-state solution of an orthotropic web which satisfies Eq (8) is assumed as:

$$u_0 = x \Delta; \quad v_0 = -\nu y \Delta; \quad \Rightarrow \quad N_{x0} = E h \Delta \quad (10)$$

where  $\Delta$  is the actual loading specified as the product of a unit loading system and a scalar load factor. To determine the transverse motion of the web in the  $y$ -direction and the Airy functions, the two sets of orthogonal functions in the sense of boundary conditions for longitudinal edges have been introduced

$$\begin{aligned} f_1 &= w; & f_3 &= w_{,\psi\psi} + \nu w_{,\xi\xi} \\ f_2 &= \frac{w_{,\eta}}{b} = w_{,\psi}; & f_4 &= E_2 (w_{,\psi\psi} + \nu w_{,\xi\xi})_{,\psi} + 4w_{,\xi\xi\psi} \end{aligned} \quad (11)$$

and

$$\begin{aligned} a_1 &= \Phi; & a_3 &= \Phi_{,\psi\psi} - \nu \Phi_{,\xi\xi} \\ a_2 &= \Phi_{,\psi}; & a_4 &= (\Phi_{,\psi\psi} - \nu \Phi_{,\xi\xi})_{,\psi} + \frac{E}{G} \Phi_{,\xi\xi\psi} \end{aligned} \quad (12)$$

$$\text{where: } \xi = \frac{x}{b}; \quad \psi = \frac{y}{b}; \quad E_1 = \frac{E}{G(1-\eta\nu^2)}; \quad E_2 = E_1 \eta \quad (13)$$

In further considerations the approximate solutions of Eq (11) has been determined by means of the series of eigenfunctions for the unmoved plate and for  $q = 0$

$$f_i = \sum_{m=1}^M \sum_{n=1}^N T_{mn}(t) F_{imn}(\psi) \sin \frac{m\pi b\xi}{l} \quad i = 1, \dots, 4 \quad (14)$$

where  $F_{imn}(\psi)$  - initially unknown function which will be determined using the transition matrix method [1] and Godunov's orthogonalization procedure,

$T_{mn}(t)$  - unknown function of time.

To determine an unknown functions  $F_{imn}(\psi)$ , after substituting (14) into (11), the linearized form of differential equilibrium equation (6) for  $c = 0$ ,  $q = 0$  and  $T_{mn}(t) = e^{j\omega_{mn}t}$  were obtained as the set of the first-order differential equations with respect to  $\psi$  (Appendix A). After substituting (11) and (12) into (7) the non-linear compatibility equation can be written as follows:

$$\begin{aligned} a_{1,\psi} &= a_2 \\ a_{2,\psi} &= a_3 + \nu a_{1,\xi\xi} \\ a_{3,\psi} &= a_4 - \frac{E}{G} a_{2,\xi\xi} \\ \frac{1}{E h \eta} (a_{1,\xi\xi\xi\xi} + \eta a_{4,\psi} - \nu \eta a_{2,\xi\xi\psi}) &= f_{2,\xi}^2 - f_{1,\xi\xi} f_{2,\psi} \end{aligned} \quad (15)$$

The exact solutions of Eq (15) one can predict in the following form:

$$\begin{aligned} a_1 &= \sum_m \sum_n \sum_i \sum_j T_{mn} T_{ij} \left[ (1 - \delta_{mi}) A_{1mnij}(\psi) \cos \frac{(m-i)\pi b \xi}{l} + \delta_{mi} A_{1mnij}(\psi) + \right. \\ &\quad \left. + A_{2mnij}(\psi) \cos \frac{(m+i)\pi b \xi}{l} \right] + N_x b^2 \frac{\psi^2}{2} \\ a_2 &= \sum_m \sum_n \sum_i \sum_j T_{mn} T_{ij} \left[ (1 - \delta_{mi}) B_{1mnij}(\psi) \cos \frac{(m-i)\pi b \xi}{l} + \delta_{mi} B_{1mnij}(\psi) + \right. \\ &\quad \left. + B_{2mnij}(\psi) \cos \frac{(m+i)\pi b \xi}{l} \right] + N_x b^2 \psi \\ a_3 &= \sum_m \sum_n \sum_i \sum_j T_{mn} T_{ij} \left[ (1 - \delta_{mi}) C_{1mnij}(\psi) \cos \frac{(m-i)\pi b \xi}{l} + \delta_{mi} C_{1mnij}(\psi) + \right. \\ &\quad \left. + C_{2mnij}(\psi) \cos \frac{(m+i)\pi b \xi}{l} \right] + N_x b^2 \\ a_4 &= \sum_m \sum_n \sum_i \sum_j T_{mn} T_{ij} \left[ (1 - \delta_{mi}) D_{1mnij}(\psi) \cos \frac{(m-i)\pi b \xi}{l} + \delta_{mi} D_{1mnij}(\psi) + \right. \\ &\quad \left. + D_{2mnij}(\psi) \cos \frac{(m+i)\pi b \xi}{l} \right] \end{aligned} \quad (16)$$

where:  $A_{1mnij} \div D_{2mnij}$  - initially unknown function of  $\psi$  which will be determined using the transition matrix method and Godunov's orthogonalization procedure,  $\delta_{mi}$  - Kronecker's delta.

Substituting Eq (16) into Eq (15) the set of the first-order differential equations with respect to  $\psi$  can be determined (Appendix B). The set of differential equations solution determines the unknown functions  $A_{1mnij} \div D_{2mnij}$ . The orthogonal functions  $f_i$  and  $a_i$  enable non-linear analysis of coupled flexural and flexural-and-torsional vibrations. After taking into considerations the sets of orthogonal functions (11) and (12) the non-linear governing equation (6) has the form

$$\begin{aligned}
& -\frac{12\rho b^2}{G h^2} (b^2 f_{1,\eta} + 2cb f_{1,\xi} + c_t b f_{1,\xi} + c^2 f_{1,\xi\xi}) - E_1 f_{1,\xi\xi\xi\xi} - \nu E_2 f_{2,\xi\xi\psi} - f_{4,\psi} + \\
& + \frac{12q b^4}{G h^3} + \frac{12}{G h^3} [a_{2,\psi} f_{1,\xi\xi} + a_{1,\xi\xi} f_{2,\psi} - 2a_{2,\xi} f_{2,\xi}] - \frac{12b^2}{G h^3} (b^2 \beta f_{1,\eta} + b\beta c f_{1,\psi}) = 0
\end{aligned} \quad (17)$$

The solutions (14) and (16) were substituted into Eq (17) and the Galerkin-Bubnov orthogonalization method has been used to find approximated solution of Eq (17). In this way the set of  $(M \times N)$  ordinary differential equations with respect to the function  $T_{kl}(t)$  can be determined in the following form

$$\begin{aligned}
& z_{0kl} \frac{d^2 T_{kl}}{dt^2} + (z_{1kl} c^2 - z_{2kl}) T_{kl} + \sum_m \sum_n r_{0mnkl} c \frac{dT_{mn}}{dt} + \sum_m \sum_n r_{1mnkl} c_{,t} T_{mn} + \\
& + \sum_m \sum_n \sum_i \sum_j \sum_p \sum_s d_{mnijpskl} T_{mn} T_{ij} T_{ps} + z_{4kl} \beta \frac{dT_{kl}}{dt} + \sum_m \sum_n r_{2mnkl} T_{mn} = -z_{3kl} q
\end{aligned} \quad (18)$$

where:  $k = 1, 2, \dots, M$ ,

$l = 1, 2, \dots, N$ .

The coefficients of the set (18) are given in Appendix C.

#### 4. Numerical results and discussion

Numerical investigations have been carried out for steel web. Parameters data: length  $l = 1\text{m}$ , width  $b = 0.2\text{ m}$ , thickness  $h = 0.0015\text{ m}$ , mass density  $\rho = 7800\text{ kg/m}^3$ , Young's modulus along  $x$   $E_x = 0.2 \cdot 10^{12}\text{ N/m}^2$ , Young's modulus along  $y$   $E_y = 0.167 \cdot 10^{12}\text{ N/m}^2$ , shear modulus  $G = 6.5 \cdot 10^{10}\text{ N/m}^2$ , Poisson's ratio  $\nu = 0.3$ , orthotropy factor  $\eta = 0.836$ , initial stress  $N_0 = 2500\text{ N/m}$ .

At first the linearized undamped system was investigated. Let  $\sigma$  and  $\omega$  denote the real part and the imaginary part of eigenvalues, respectively. The positive value of  $\sigma$  indicates instability of the system and  $\omega$  is natural frequency of the web. To show dynamic behaviour of the web the lowest three flexural (solid line) and two flexural-and-torsional (dotted line) natural frequencies plots versus transport velocity  $c$  are shown in Fig.2. In supercritical transport speeds ( $c > c_{cr1}$ ) at first the web experiences divergent instability (the fundamental mode with non-zero  $\sigma$  and zero  $\omega$ ) and next flutter instability (non-zero  $\sigma$  and non-zero  $\omega$ ). The second critical transport speed is denoted by  $c_{cr2}$ . Between these two instability regions there is a second stability area where  $\sigma = 0$ . The width and position of the second stable region are dependent on the orthotropy factor of the web. The plot of the lowest transverse eigenfrequencies for various values of the orthotropy factor  $\eta$  are shown in Fig.3

Next the non-linear damped model of the steel web was investigated. In undercritical region of transport speeds ( $c < c_{cr1}$ ) one can observe free flexural vibrations around trivial equilibrium position (Fig.4). Comparison of the linear and non-linear solutions for fundamental eigenfrequency shows the linear theory underestimates stability of the web motion in subcritical range of transport speeds (Fig5)



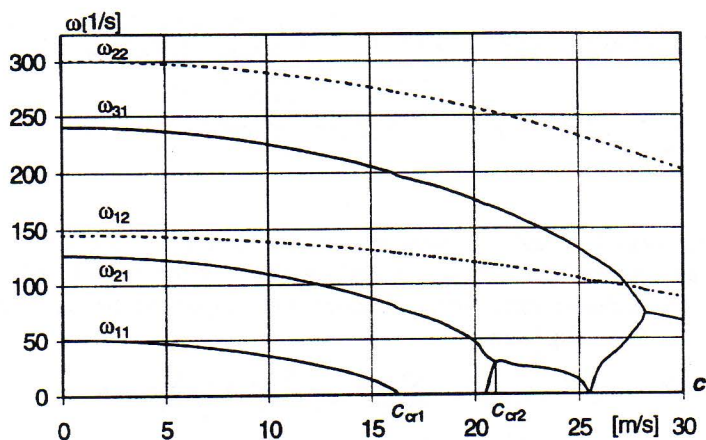


Fig.2. The lowest natural frequencies of the web.

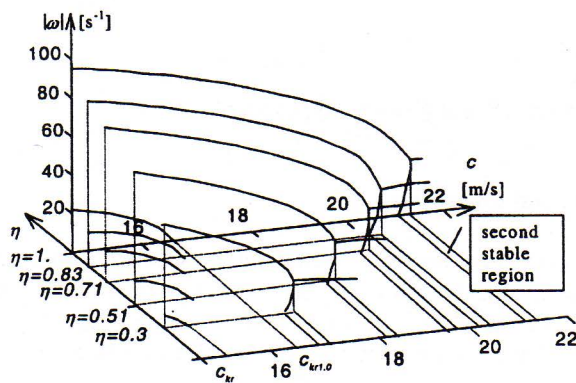
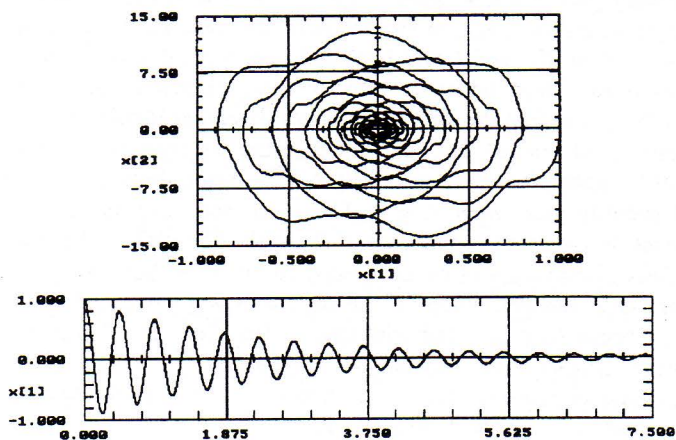


Fig.3. The lowest flexural eigenfrequencies of the web.

Fig.4. The phase (a) and flexural vibrations (b) plots ( $c = 15 \text{ m/s}$ ,  $\beta = 10 \text{ kg m}^{-2} \text{ s}^{-1}$ ).

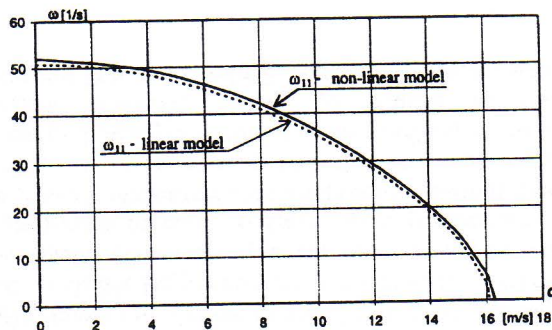


Fig.5. Comparison of the linear and non-linear fundamental eigenfrequency.

Numerical results in the form of the phase and transverse vibrations diagrams in various supercritical transport speed of the web are shown in Fig.6 and Fig.7. Though the analysis of the linearized system predicts exponentially growing oscillations in divergence instability region of transport speeds, non-linear damped vibrations which tend to new equilibrium position occur (Fig.6). Above the second critical speed of the linearized system the non-linear system experiences global motion between new equilibrium positions (Fig.7)

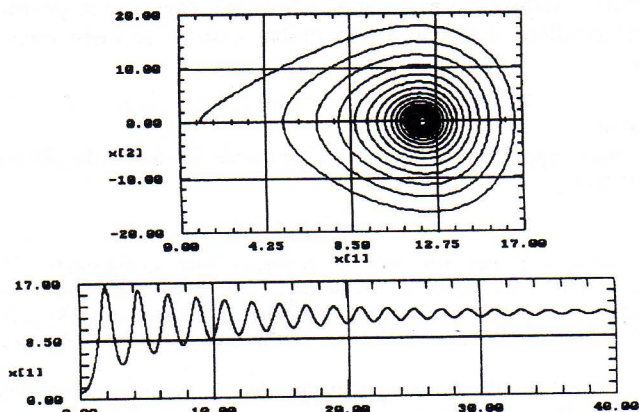


Fig.6. The phase (a) and flexural vibrations (b) plots ( $c = 16.2$  m/s,  $\beta = 2$  kg m<sup>-2</sup> s<sup>-1</sup>).

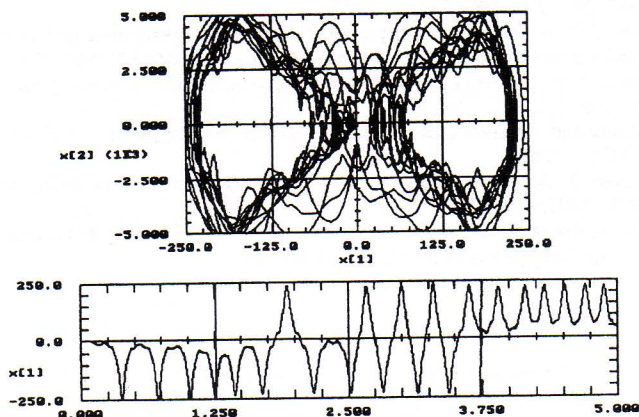


Fig.7. The phase (a) and flexural vibrations (b) plots ( $c = 21.5$  m/s,  $\beta = 1$  kg m<sup>-2</sup> s<sup>-1</sup>).

## 5. Conclusions

In the paper a new method of dynamic analysis of axially moving orthotropic web is presented. The numerical method of Unger's transition matrix and Godunov's orthogonalization procedure are used to solve the non-linear problem of axially moving system. The results of numerical investigations show the solutions of the linearized and non-linear problems. Numerical investigations have been carried out for steal web.

The linearized mathematical model analysis shows in subcritical region of transport speed for the constant axial tension of the web the lowest transverse natural frequency decreases during the axial velocity increase. At first critical transport speed the fundamental eigenfrequency vanishes indicating divergence instability. In supercritical region of transport speed at first the web experiences divergent instability and next flutter instability above the second critical speed. The second stable region of the linearized system may appears above the first critical transport speed. The critical transport speed value and the position of the second stability region are dependent on the orthotropy factor of the web. In the range  $\eta < 1$  the orthotropy factor decreasing diminishes the critical axial speed

Comparison of the linear and non-linear solutions for fundamental eigenfrequency shows the linear theory underestimates stability of the web motion in subcritical range of transport speeds. Dynamic analysis of the non-linear damped system with constant axial stress shows in supercritical transport speed region non-trivial equilibrium positions bifurcate from the straight configuration of the web and global motion between coexisting equilibrium positions occurs.

## Acknowledgement

This paper was supported by the State Committee for Scientific Research (KBN) under grant No. 7 T08E 034 17.

## References

- [1] Unger B.: Elastisches Kippen von beliebig gelagerten und aufgehängten Durchlaufträgern mit einfachsymmetrischen, in Trägerachse veränderlichem Querschnitt und einer Abwandlung des Reduktionsverfahrens als Lösungsmethode, *Dissertation D17*, Darmstadt 1969.
- [2] Wang X.: Numerical Analysis of Moving Orthotropic Thin Plates, *Computers & Structures*, **70**, 1999, 467 - 486.
- [3] Wickert J.A., Mote C.D. Jr: Current research on the vibration and stability of axially moving materials. *Shock and Vibration Digest* **20**, 1988, 3 - 13.
- [4] Wickert J.A., Mote C.D. Jr: Classical vibration analysis of axially moving continua. *Journal of Applied Mechanics ASME* **57**, 1990, 738 - 744.
- [5] Lin C.C., Mote C.D. Jr: Equilibrium displacement and stress distribution in a two dimensional, axially moving web under transverse loading. *J. of Applied Mechanics ASME* **62**, 1995, 772-779.
- [6] Lin C.C., Mote C.D. Jr: The wrinkling of thin, flat, rectangular webs. *Journal of Applied Mechanics ASME* **63**, 1996, 774 - 779.
- [7] Lin C.C.: Stability and vibration characteristics of axially moving plates. *Int. Journal of Solid Structures* **34**(24), 1997, 3179 - 3190,
- [8] Moon J., Wickert J. A.: Non-Linear Vibration of Power Transmission Belts, *Journal of Sound and Vibration*, **200**(4), 1997, 419 - 431.
- [9] Marynowski K., Kołakowski Z.: Dynamic behaviour of an axially moving thin orthotropic plate. *Journal of Theoretical and Applied Mechanics* **37**(1), 1999, 109 - 128.



## Appendix A

The linearized form of differential equilibrium equations:

$$\begin{aligned}
 \frac{dF_{1mn}}{d\psi} &= F_{2mn}; \\
 \frac{dF_{2mn}}{d\psi} &= F_{3mn} + \nu F_{1mn} \left( \frac{m\pi b}{l} \right)^2; \\
 \frac{dF_{3mn}}{d\psi} &= \frac{1}{E_2} \left[ F_{4mn} + 4 \left( \frac{m\pi b}{l} \right)^2 F_{2mn} \right] \\
 \frac{dF_{4mn}}{d\psi} &= -E_1 F_{1mn} \left( \frac{m\pi b}{l} \right)^4 + \nu E_2 \frac{dF_{2mn}}{d\psi} \left( \frac{m\pi b}{l} \right)^2 + \\
 &\quad + \frac{2b^2 \rho h}{D_1} F_{1mn} b^2 \omega_{mn}^2 - \frac{12b^2}{h^2} F_{1mn} \left( \frac{m\pi b}{l} \right)^2 E_1 (1 - \eta \nu^2) \Delta
 \end{aligned} \tag{A.1}$$

where:  $\omega_{mn}$  - the eigenfunction of the linearized system.

## Appendix B

The set of the first-order differential equations with respect to  $\psi$ :

$$\begin{aligned}
 \frac{dA_{1mnij}}{d\psi} &= B_{1mnij}; \quad \frac{dA_{2mnij}}{d\psi} = B_{2mnij} \\
 \frac{dB_{1mnij}}{d\psi} &= C_{1mnij} - \delta_{mi} \nu A_{1mnij} \left[ \frac{(m-i)\pi b}{l} \right]^2; \\
 \frac{dB_{2mnij}}{d\psi} &= C_{2mnij} - \nu A_{2mnij} \left[ \frac{(m+i)\pi b}{l} \right]^2; \\
 \frac{dC_{1mnij}}{d\psi} &= D_{1mnij} + \delta_{mi} \frac{E}{G} B_{1mnij} \left[ \frac{(m-i)\pi b}{l} \right]^2; \\
 \frac{dC_{2mnij}}{d\psi} &= D_{2mnij} + \frac{E}{G} B_{2mnij} \left[ \frac{(m+i)\pi b}{l} \right]^2; \\
 \frac{dD_{1mnij}}{d\psi} &= \delta_{mn} \left\{ -\frac{A_{1mnij}}{\eta} \left[ \frac{(m-i)\pi b}{l} \right]^4 - \nu \frac{dB_{1mnij}}{d\psi} \left[ \frac{(m-i)\pi b}{l} \right]^2 \right\} + \\
 &\quad + \frac{Eh}{2} \left[ F_{2mn} F_{2ij} \left( \frac{m\pi b}{l} \right) \left( \frac{i\pi b}{l} \right) + F_{1mn} \frac{dF_{2ij}}{d\psi} \left( \frac{m\pi b}{l} \right)^2 \right] \\
 \frac{dD_{2mnij}}{d\psi} &= \left\{ -\frac{A_{2mnij}}{\eta} \left[ \frac{(m+i)\pi b}{l} \right]^4 - \nu \frac{dB_{2mnij}}{d\psi} \left[ \frac{(m+i)\pi b}{l} \right]^2 \right\} + \\
 &\quad + \frac{Eh}{2} \left[ F_{2mn} F_{2ij} \left( \frac{m\pi b}{l} \right) \left( \frac{i\pi b}{l} \right) - F_{1mn} \frac{dF_{2ij}}{d\psi} \left( \frac{m\pi b}{l} \right)^2 \right]
 \end{aligned} \tag{A.2}$$

### Appendix C

The coefficients of the set (18):

$$\begin{aligned}
 z_{0kl} &= -\iint \frac{12\rho b^4}{Gh^2} F_{1kl}^2 \sin^2 \frac{k\pi b\xi}{l} d\xi d\psi; \\
 z_{1kl} &= \iint \frac{12\rho b^2}{Gh^2} F_{1kl}^2 \left(\frac{k\pi b}{l}\right)^2 \sin^2 \frac{k\pi b\xi}{l} d\xi d\psi; \\
 z_{2kl} &= \frac{z_{1kl} b^2 \omega_{kl}^2}{\left(\frac{k\pi b}{l}\right)^2}, \quad z_{3kl} = \iint \frac{12b^4}{Gh^3} F_{1kl} \sin \frac{k\pi b\xi}{l} d\xi d\psi; \\
 z_{4kl} &= -\iint \frac{12b^4}{Gh^3} F_{1kl}^2 \sin^2 \frac{k\pi b\xi}{l} d\xi d\psi;
 \end{aligned} \tag{A.3}$$